

‘OHANA*

Guy Perrin^{†a}, Olivier Lai^b, Julien Woillez^c, Jean Guerin^a, Takayuki Kotani^a, Sébastien Vergnole^d,
Andy J. Adamson^e, Christ Ftaclas^f, Olivier Guyon^g, Pierre Léna^a, Jun Nishikawa^h, François
Reynaud^d, Kathy Rothⁱ, Stephen T. Ridgway^{a,j}, Alan T. Tokunaga^k, Peter L. Wizinowich^c,

^a LESIA, Observatoire de Paris, 5 place Jules Janssen, 92190 France ;

^b Canada France Hawai'i Telescope, PO Box 1597, Kamuela, HI 96743, USA ;

^c W.M. Keck Observatory, 65-1120 Mamalahoa Hwy, Kamuela, HI 96743, USA ;

^d IRCOM, 123, avenue Albert Thomas, 87060 Limoges CEDEX, France ;

^e United Kingdom Infrared Telescope, Joint Astronomy Centre, 660 N. A'ohoku Place, University
Park, Hilo, HI 96720, USA ;

^f Institute for Astronomy, University of Hawai'i, 2680 Woodlawn Drive, Honolulu, HI 96822, USA ;

^g Subaru Telescope, 650 North A'ohoku Place, Hilo, 96720 HI, USA ;

^h National Astronomical Observatory, Mitaka, 2-21-1 Osawa, Mitaka, Tokyo, Japan 181-8588 ;

ⁱ Gemini Observatory, Northern Operations Center, 670 N. A'ohoku Place, Hilo, HI 96720, USA ;

^j Kitt Peak National Observatory, National Optical Astronomy Observatories, PO Box 26732,
Tucson, AZ 85726, USA ;

^k IRTF, Institute for Astronomy, University of Hawai'i, 2680 Woodlawn Drive, Honolulu, HI 96822,
USA

ABSTRACT

The Mauna Kea Observatory offers a unique opportunity to build a large and sensitive interferometer. Seven telescopes have diameters larger than 3 meters and are or may be equipped with adaptive optics systems to correct phase perturbations induced by atmospheric turbulence. The maximum telescope separation of 800 meters can provide an angular resolution as good as 0.25 milli-arcseconds in the J band. The large pupils and long baselines make ‘OHANA very complementary to existing large optical interferometers. From an astrophysical point of view, it opens the way to imaging of the central part of faint and compact objects such as active galactic nuclei and young stellar objects. On a technical point of view, it opens the way to kilometeric or more arrays by propagating light in single-mode fibers. First instruments have been built and tested successfully at CFHT, Keck I and Gemini to inject light into single-mode fibers thus partly completing Phase I of the project. Phase II is now on-going with the prospects of the first combinations of Keck I - Keck II in 2004 and Gemini - CFHT in 2005.

Keywords: Interferometry, ‘OHANA, Single-mode fiber, Adaptive Optics

1. INTRODUCTION

* Copyright 2004 Society of Photo-Optical Instrumentation Engineers (SPIE). This paper was (will be) published in *New Frontiers in Stellar Interferometry*, W. A. Traub, ed., SPIE Proceedings Series, Vol. 5491, paper [5491-43], and is made available as an electronic reprint (preprint) with permission of SPIE. One print or electronic copy may be made for personal use only. Systematic or multiple reproduction, distribution to multiple locations via electronic or other means, duplication of any material in this paper for a fee or for commercial purposes, or modification of the content of the paper are prohibited.

[†] guy.perrin@obspm.fr

The ‘OHANA project consists in linking the large telescopes of the Mauna Kea summit with single-mode fiber optics to realize a large near-infrared interferometer. The idea was first published by Mariotti et al. (1996)¹. The project started in 2000 and has been described in its current version in Perrin et al. (2000)². ‘OHANA is a quite ambitious and new type of interferometer. Several phases are therefore necessary before a full combination of the Mauna Kea telescopes can be achieved. This is why the project has been divided into three phases. A first phase to build and optimize the instruments required to inject light into single-mode fibers at the focus of the adaptive optics systems. This phase has been a success and is described in details in Woillez et al. (2004)³. In the second phase, the “shortest” baselines will be linked to demonstrate the concept of ‘OHANA. Once it is believed that ‘OHANA can be operated to produce very valuable astrophysical results, the full array may be built and operated as described in Lai et al. (2002)⁴. The goals of the current project are various. Demonstrate the potential of single-mode fiber technology for kilometeric and deca-kilometeric arrays. Demonstrate the sensitivity of interferometers making use of both large pupils corrected with AO and single-mode fibers for coherent transport of light. Reach below 1 mas angular resolution in the near-infrared. Make the astrophysical interest of such an instrument clear. We present the current status of project in this paper.

2. OVERVIEW OF THE WHOLE PROJECT

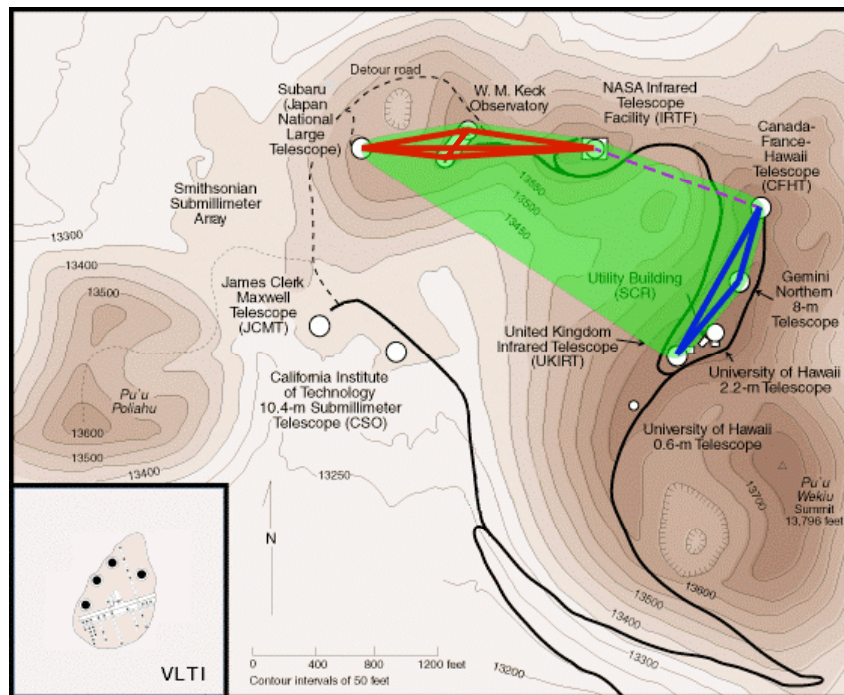


Figure 1: Map of the Mauna Kea summit. The red and blue lines represent the ‘OHANA Phase II baselines. The green area is the future Phase III full ‘OHANA array. The dashed purple line connects CFHT to IRTF, a possible although very difficult baseline for Phase II. In the bottom left corner, VLTI is represented at the same scale.

Figure 1 shows a map of the Mauna Kea observatory. The solid and dashed lines are the baselines conceivable during Phase II. Except for the Keck telescopes, none of the other telescopes have been designed to be used interferometrically. As a consequence they are not equipped with facilities to equalize the optical paths which therefore has to be done. Because of the telescopes lay-out on the mountain, it is possible to distinguish two groups of telescopes: the telescopes roughly aligned in a North-South direction as UKIRT, Gemini and CFHT, and the telescopes aligned in an East-West direction as Subaru, Keck I&II and IRTF. It is very fortunate that the Keck telescopes are situated in the middle of the East-West complex. As a matter of fact, it is very difficult to find and track fringes on an East-West baseline because of the fast sidereal motion of the fringes and this requires very good and efficient delay lines. The Keck interferometer delay lines are therefore ideally suited for these baselines. On the other side, a dedicated delay-line has to be fabricated

for the quasi North-South baselines. This delay line will first be located in the CFHT Coudé room for the coupling of Gemini and CFHT. The delay line is described in Section 6. The IRTF-CFHT baseline is represented by a dashed line as it is not sure yet that either enough lengths of fibers or suitable delay lines will be available in Phase II. These baselines altogether provide a very good coverage in azimuth in spatial frequency space. The green area represents the baselines achievable in Phase III when the longest baseline (Gemini-Subaru, 756 m) will provide the highest spatial resolution.

The table below lists the baseline lengths and the spatial resolutions in the J, H and K bands. The colours are matched to that of the groups of baselines on the figure above. All baselines are longer than what both the Keck interferometer and the VLTI can provide at equivalent sensitivity. ‘OHANA will therefore be a good complement to these two projects and it will extend their resolving power by a factor of 5 at equivalent sensitivity. Due to the supersynthesis effect, objects of a fraction of 0.1 mas will be resolved by the interferometer.

Baseline	Length (m)	Resolution (mas)		
		J	H	K
Keck I – Subaru	147	1.75	2.32	3.09
Keck II – Subaru	222	1.16	1.53	2.05
IRTF – Keck II	237	1.09	1.43	1.91
IRTF – Keck I	287	0.90	1.19	1.58
Keck I – Keck II	85	3.03	4.00	5.34
IRTF – Subaru	430	0.60	0.79	1.06
CFHT-IRTF	344	0.75	0.99	1.32
CFHT-Gemini	162	1.59	2.10	2.80
UKIRT-Gemini	202	1.28	1.68	2.25
CFHT-UKIRT	347	0.74	0.98	1.31
Gemini-IRTF	410	0.63	0.83	1.11
UKIRT-IRTF	455	0.57	0.75	1.00
CFHT-Keck II	580	0.44	0.59	0.78
UKIRT-Keck I	604	0.43	0.56	0.75
UKIRT-Keck II	615	0.42	0.55	0.74
CFHT-Keck I	617	0.42	0.55	0.74
Gemini-Keck II	624	0.41	0.55	0.73
Gemini-Keck I	641	0.40	0.53	0.71
UKIRT-Subaru	689	0.37	0.49	0.66
CFHT-Subaru	750	0.34	0.45	0.60
Gemini-Subaru	756	0.34	0.45	0.60

3. PRINCIPLE OF THE ‘OHANA INTERFEROMETER

The main characteristic of ‘OHANA is the use of single-mode fibers to route the beams between telescopes. All other existing interferometers make use of classical optics to direct the beams from the telescope foci to the beam combiner. ‘OHANA is addressing a novel technique in which most of beam trains are replaced by single-mode fibers. With the current technology however it is not yet possible to build long enough delays in fibers. Delays of 2 m have been achieved by stretching silica fibers⁵. Fibers being dispersive media, unbalanced pathlengths generate longitudinal dispersion thus reducing the fringe contrast unless the bandwidth is reduced and as a consequence the number of photons. Photonic crystal fibers (PCF) have the potential to have zero dispersion and may offer a solution to this issue when this technology will have reached enough maturity for astronomical interferometry. First tests show that these new types of single-mode fibers can be used for interferometry⁶. Classical delay lines need to be used instead.

Single-mode fibers offer several potential advantages. First of all, in the case of the Mauna Kea submit, they allow to combine existing telescopes to build a large interferometer without requiring the construction of new facilities. As will

be addressed in Section 5, single-mode fibers have high transmissions and should help build sensitive interferometers. When compared to classical optics interferometers suffering from reflexion, diffusion and diffraction losses, single-mode fibers should be highly efficient for very long baseline interferometers in the near-infrared. Last but not least, the entire coherence of beams is preserved in single-mode fibers and spurious effects such as turbulence losses are filtered at the fiber input head thus ensuring maximum coherence and therefore maximum fringe contrast.

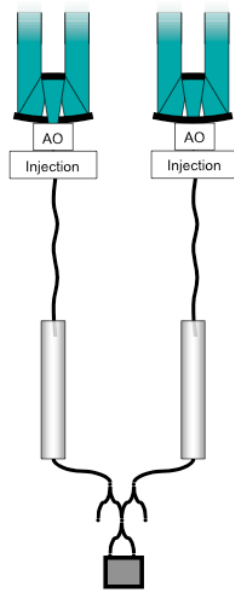


Figure 2: Principle of the ‘OHANA interferometer (Phase II). The coherent flux is injected at the adaptive optics corrected telescope foci with sub-systems called injection modules. Photons are routed to the delay lines (white cylinders) in single-mode fibers. Delay lines are made with classical optics. Beams are injected in fibers again at the output of the delay lines and mixed in the beam combiner.

Fibers are the main driver for the ‘OHANA interferometer. The concept is illustrated on Figure 2. Fluxes collected by the telescopes are focused into single-mode fibers using subsystems baptized “injection modules”. Given the diameter of single-mode fibers, from 5 μm in the J band to 6.5 μm in the K band, it is mandatory that beams be corrected from static and turbulent aberrations induced by the atmosphere with adaptive optics systems. Insuring maximum efficiency injections in single-mode fibers is equivalent to maximizing the coherence of beams in classical interferometry. Injected photons are propagated towards delay lines in chromatic dispersion matched fibers. Delay lines are classical free-space propagation systems. In Phase II, ‘OHANA combines pairs of telescopes. The beam combiner is an evolution of the FLUOR beam combiner. In FLUOR-like single-mode interferometers, turbulence-induced phase fluctuations are traded against coupling fluctuations which can be monitored in real-time and used to calibrate interferograms thus cancelling coherence errors due to turbulence. The ‘OHANA beam combiner also applies this principle but in a different manner. Instead of using a cascade of couplers for beam sampling, a spatial modulation is used to provide the instantaneous intensities of the beams. The principle of the beam combiner is described in more details in Section 7. In Phase III, as more than 2 telescopes if not all will be used simultaneously, the beam combiner will combine more than 2 beams and will provide phase closures.

4. INJECTION MODULES - PHASE I

The experiments of Phase I are described in more details in Woillez et al. (2004)³. The goals of these experiments was twofold. Firstly, concentrate during a non-interferometric phase on the problem of injecting light in single-mode fibers in

a timely efficient way as this operation should be quick in the interferometric phase. Secondly, demonstrate that the amount of injected flux will be sufficient for 'OHANA in Phase II.

Optically, the task of the injection module is to match the field pattern of the fiber with that of the telescope. For a perfectly round telescope with no central obscuration, the squared modulus of the field is the Airy pattern. The fiber field pattern can be approximated by a gaussian. The fields are therefore different but optimum match -- or injection -- is obtained when, to the first order, the FWHMs of the two patterns match. In practice, the injection module will adapt the f-ratio of the telescope to that of the fiber, about 3. In conditions free of aberrations and for perfectly circular and full pupils, the maximum coupling ratio is about 80%. The central obscuration of telescopes and their particular shapes will decrease this maximum coupling ratio. Down to 40% in the case of the CFHT whose central obscuration is large (1.20 m in diameter). Atmospheric turbulence will further reduce the coupling efficiency. Strehl ratios of 60% are usually expected in the K band. In the case of the CFHT, for example, the maximum coupling ratio should therefore not exceed 24% and be about 50% with the Keck. Other factors may degrade it: the intrinsic aberrations of the injection module, non perfect alignments, non-optimum f-ratios (the three bands, J, H and K do not have the same optimum f-ratio), potential bad seeing conditions, centering errors of the fiber with respect to the diffraction pattern of the telescope.

Tests have been undertaken at CFHT (July-August 2002), Keck I (December 2002) and Gemini (July 2003). The same module has been used for the three telescopes with the required specificities for each (parabolas, mounting interfaces). Tests at CFHT and Gemini were performed at the Cassegrain foci whereas the module was set-up at the Nasmyth focus of Keck I. Stiffness of the module was such that flexures were no more than two Airy patterns at K in the image plane thus ensuring great pointing stabilities. This constraint was fully relaxed in the case of Keck I as gravity was always perpendicular to the module and no flexures were to be feared. Knowledge of the module and injection efficiency have improved from one run to another. Unfortunately, the last run at Gemini was severely hampered by bad weather and no calibration of the injection efficiency was possible. The average coupling ratio recorded at CFHT was slightly less than 10% during the second night but was however as high as 20% which was close to the expected maximum of 24%. Injection tests at Keck I suffered from high winds causing telescope shaking in the second night. Despite this, maximum injections has high as 50% were recorded.

In conclusion, it turns out that coupling efficiencies of 10% should be the average baseline to assess the sensitivity of 'OHANA. Although this may seem small relative to the ideal case, it seems reasonable when considering the limitations due to the optics and to the effect of turbulence. In any case, this provides enough flux for efficient testing of 'OHANA in Phase II and for valuable scientific results. The 10% efficiency was the figure used in Perrin et al. (2000)² to derive the sensitivity of the instrument.

5. FIBERS

'OHANA will use two kinds of single-mode fibers: silica and fluoride glass fibers. The silica fibers will be used for the J and H bands whereas the fluoride glass fibers will give access to the K band. The losses of these fibers are potentially in the range 0.1-0.2 dB/km for the silica fibers and 1-2 dB/km for the fluoride glass fibers, 3 dB meaning a loss of 50% of the photons. Connectors between fibers have losses of 0.1 dB. Fiber links are therefore a promising technique for long baseline interferometers.

The maximum loss caused by propagation in the fibers is therefore of 1dB at most for baselines up to 450 m. However, in order to balance dispersion of the fiber pairs and for practical reasons, each fiber link is an assembling of 50 m sections in K and of 100 m and 200 m sections in J and H. The transmission of the 300 m K band fibers is 50% with space for improvement. The J and H band 300 m fiber links have transmissions of 90%. A conservative value of the transmission is of 50% which is very competitive compared to classical optical trains. Besides, transmission and coherence losses created by diffraction effects disappear in fibered links. Yet, bulk optics will have to be used for the delay lines as long delays cannot be produced by stretching fibers without creating differential dispersion. Extra losses will therefore occur when getting out and back into the fibers.

Fibers are dispersive media and this point has been addressed cautiously to build the interferometer. It is basically impossible as of today to cancel intrinsic dispersion in fibers as this requires to master the waveguide design to within a

terrific precision (on the order of a few nanometers on the core size for example). Photonic Cristal Fibers are very promising in this respect but constraints remain very stringent⁶. In order to balance dispersion in fiber pairs, the technique consists in adjusting the fiber lengths and choosing the fiber cables so that intrinsic dispersions are matched in the two lengths of fibers in the interferometer. This has proved to be efficient on fibers a few meters long where the dominant effect (second order) can be cancelled by adjusting the respective lengths of the fibers. For longer fiber lengths, the second order of dispersion can still be adjusted with this technique but the third order is no more negligible. The third order is basically generated by the variation of the core diameter along fiber cables which is difficult to avoid for long lengths. The third order can be cancelled by breaking a long fiber into shorter fibers a few tens or a hundred meters long and by choosing the best combination. This requires to produce long lengths of fibers and to make a selection. This is efficient to reduce dispersion but requires more connections and causes losses. This technique has been applied for the K band fluoride-glas fibers whose individual sections are generally 50 m long. The J and H band silica fibers are made of a 200 m and a 100 m section. The third order of dispersion has been cancelled for the J and K bands but the H band fibers still have a residual third order. The second order has almost been perfectly cancelled.

Figure 3 shows the results obtained in the K' band. 6 fringes are measured at half maximum as expected. Asymmetries of the interferogram however disclose dispersion residuals difficult to compensate. But these have a very low impact on the fringe contrast as values as high as 98% have been measured⁷.

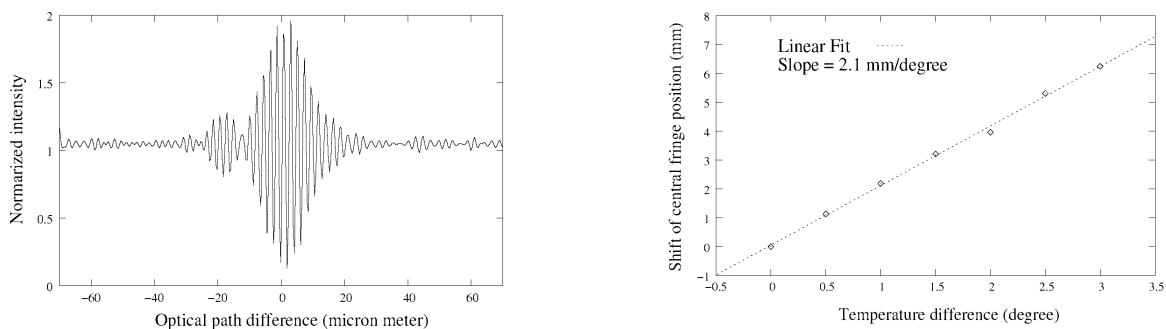


Figure 3: K band 300 m fluoride glass fibers. Left: interferogram in the K' band. 6 fringes are measured at half-maximum as expected. Asymmetries are hints of residual dispersion. Fringe contrasts as high as 98% have been obtained. Right: sensitivity of fluoride glass fibers to temperature. The temperature of 150 m of fibers of one of the interferometric arms is varied. A shift of the fringe pattern of 2.1 mm/°C is measured. This shift is induced by a contraction/expansion of the fiber which also causes dispersion.

The equivalent result in the J band is displayed in Figure 4. 8 fringes are measured at half maximum instead of 5 due to a slight dispersion residual. Asymmetries are however smaller than in the K band and dispersion residuals are comparable. High contrasts have also been measured, up to 90%⁸.

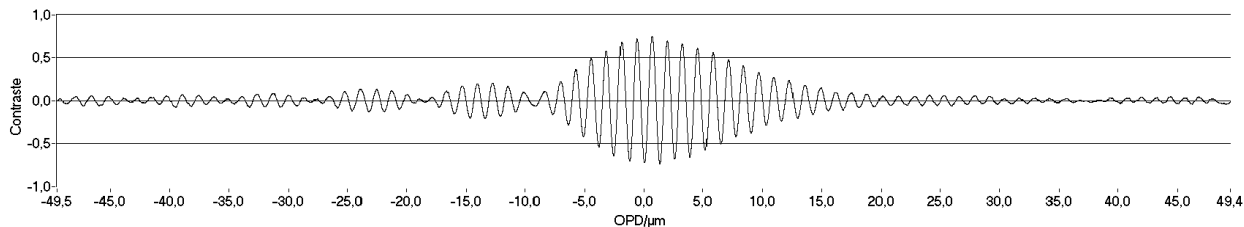


Figure 4: J band 300 m silica fibers. 8 fringes are measured at half maximum instead of 5 due to a slight residual dispersion. Maximum contrast measured: 90%.

Aside from communications, one of the uses of single-mode fibers is for temperature sensors. In other words, fibers are very sensitive to temperature, a disadvantage for interferometry when fibers linking distant telescopes lay in places with different and varying temperatures. Figure 3 gives the fringe drift measured in a lab experiment with the K band fibers⁷. 150 m of fibers of one of the interferometric arms have undergone temperature variations. A fringe pattern drift of 2.1 mm/°C has been measured. The law is perfectly linear and the sensitivity with temperature linearly varies with fiber length meaning that a 1 km long fiber interferometer would have a fringe drift of 14 mm per homogeneous differential degree of temperature. Measurements have been done with the J band fibers and lead to comparable results. The effect of temperature is not only a fringe drift. As the material expands with increasing temperature, the glass path increases and so the dispersion. Several solutions exist to counter this effect. The first one, a radical solution, consists in servoing the temperature of fibers. This active solution would be too heavy to set-up in the framework of the current prototype project but is to be considered as an efficient solution for the future. Another solution is to bury the fibers into the ground at sufficient depth where temperature is stable. This is also an attractive solution. A third solution consists in compensating temperature drifts causing dilatation or contraction of fibers by adjusting a variable thickness of glass. This has been successfully implemented with two CaF₂ wedges whose dispersion characteristics quasi perfectly match those of J and K band fibers (see Kotani et al. 2004⁴ for tests in the K band). A different glass has to be found for the H band fiber. Yet, a piezo-actuated delay line can be used in this case and has been tested in the J band as an alternative to using bulk-optics type glass. The mechanical stretching of the fiber will compensate the stretching induced by temperature. The technique to compensate temperature-induced dispersion will be as follows. Given that temperature drifts are slow, fringes will be measured in autocollimation to adjust the dispersion compensator. This adjustment will be kept for several hours on the sky to measure fringes until a dispersion increase is measured.

Another matter of concern to address are polarization effects. We use polarization maintaining fibers in the J and H bands. One of the polarizations is filtered to detect fringes as the two linear polarizations do not travel at the same velocity hence the interferograms are not synchronized and need to be separated. Besides, dispersion has been compensated on a single axis⁸. Standard fibers have to be used in the K band as no such components are available for long distance links. Yet, fluoride glass fibers have a very small birefringence so that polarization effects amount to a differential rotation of the polarization axes which can be compensated by twisting the fibers. This is how we have obtained large visibility contrasts in the lab experiment with the 'OHANA fiber and on the sky with FLUOR. To our surprise, polarization rotation has not been a problem over such fiber lengths. We have not investigated that in detail but it seems that torsions are diluted along long cable lengths, a very favorable characteristic for 'OHANA.

The fibers used for 'OHANA are protected with flexible cables. They will be plugged-in at the foci of the injection modules and will run to the telescopes enclosures housing the delay lines and the beam combining systems. For the very first baselines of Phase II, fibers can be put on the ground and will possibly be buried in the ground at moderate depth. In the case of the Keck I – Keck II combination fibers will remain in the twin telescope enclosure and no temperature effect should be feared. In later stages of Phase II, they will have to be pulled from existing ducts used for phone and network cables between telescopes. The same sets of fibers will be used for all the baselines. For the shortest baselines, 300 m of fibers are required for a focus-to-beam combiner connection. 2x500 m of fibers per band will be enough to realize all the baselines (but observations cannot be done simultaneously with different baselines).

6. DELAY LINES

Delay lines are a critical issue at Mauna Kea. No extra building can be built for 'OHANA forbidding the realization of new Keck-like delay lines. Fortunately, Keck is part of the array and provides a solution for the baselines including telescopes nearby Keck and the Keck telescopes (red baselines on Figure 1). For the western part of the array, baselines are quasi North-South oriented hence the fringe speed remains under 20 mm/s even on the longest UKIRT-CFHT baseline. A simple system can be designed to provide enough delay and track the fringes for the UKIRT-Gemini-CFHT baselines. It is a three stage system represented on Figure 5. The beams are output from the fibers with off-axis parabolas and relayed by flat and dihedral mirrors to off-axis parabolas where they are refocused in fibers. A gross delay is produced by two dihedrals mounted on a translation stage common to the two beams (two dihedrals per beam) allowing to produce +/- the maximum stroke of delay (+/- 50 m). With the four-pass system, the translation of the dihedrals will produce a delay four times larger than the extension of the carriage thus not requiring more than 13 meters of space. This four dihedral carriage will be set still during observations. An extra offset in delay can be produced if necessary by

putting one of the input or output parabolas within a fixed distance of their nominal position to shift the zero optical path difference. This will allow to extend the sky coverage.

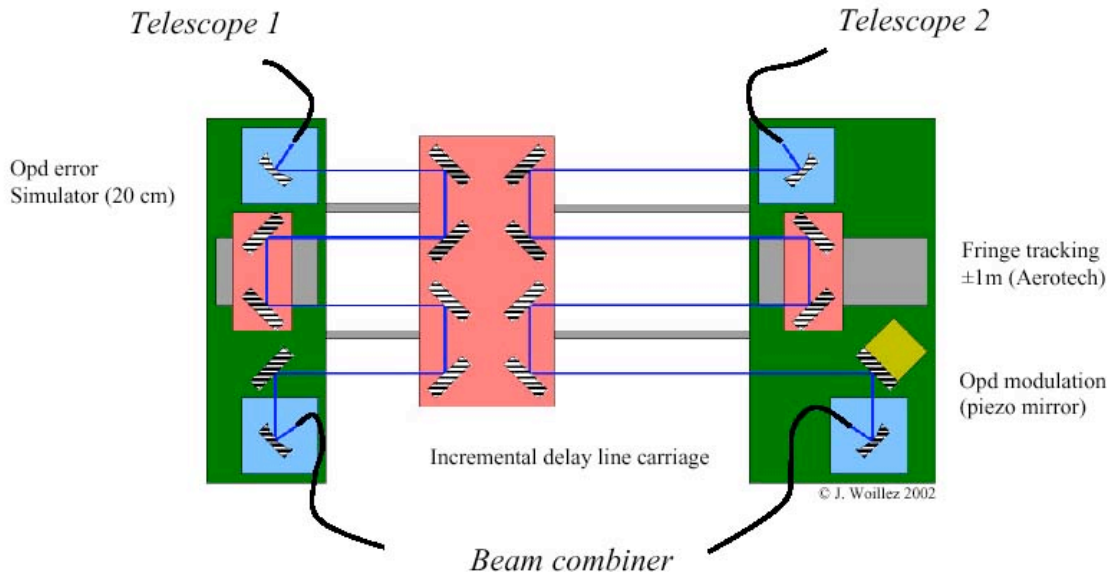


Figure 5: delay line concept for the Phase II of 'OHANA. The two J, H and K single-mode fiber bundles coming from telescopes 1 and 2 are connected at the focus of an off-axis parabola. The collimated beams are then reflected by three di-hedrals and focused again in single-mode fibers connected to the beam combiner. The delay line is a three stage system. The central carriage is moved between observations to compensate for the gross of the delay. It pushes in one arm and pulls in the other. The fringe tracking delay line follows the natural fringe drift during an observation and the flat mirror actuated by a piezo scans through fringe packets. The opd error simulator is used to simulate a fringe drift during test phases. The total stroke of the delay line is 50 meter.

Fringes will be tracked with a fast dihedral mounted on a commercial 1m-stroke translation stage from Aerotech in one of the arms of the interferometer. Tests of the Aerotech carriage have demonstrated its ability to track fringes with velocities up to 20 mm/s without too much speed jitter. In the same arm, a flat mirror is mounted on a piezo-stage to produce the modulation of the fringe packet. In the other arm, the third dihedral sits on a short stroke translation stage used to simulate baseline errors to exercise fringe tracking.

We have chosen a mechanical metrology system for the central carriage already in use at the GI2T interferometer to measure baseline lengths between relocatable telescopes. It does not require accurate alignment as for highly accurate laser metrology systems. The price to pay is a 100 μm accuracy which is actually enough given the spectral resolution of the beam combiner which provides coherence lengths on the order of 100 μm. After moving the central carriage, fringe finding will therefore take a few seconds.

This system is designed to be quickly reconfigurable. Prior to each relocation of the central carriage, the mirrors' attitude is characterized by a control system which is slid in the beam. After translation of the carriage, the carriage attitude is corrected to match the adjustment measured by the control system. No manual operation is required.

First alignments have started in Meudon as Figure 6 shows. After alignment of the rails, a straightness of +/- 1 mm has been achieved and is according to specifications. Dihedrals have been mounted and aligned. The next step is the installation of the off-axis parabolas and of the fiber positioners. Eventually, the control system will allow the first operational tests in the second half of 2004.

The delay line is primarily designed for the Gemini-CFHT baseline and it will be installed in the CFHT Coudé room in 2005. Other designs have been proposed for longer baselines by Ridgway et al. (2002)⁹.



Figure 6: Views of the delay line during the integration phase in Meudon. Left: mechanical structure in the integration tunnel before integration of optics. The translation stage on the front optical table is the Aerotech 1 m stroke stage. The total length of the delay line is 14 m. Right : view of the central carriage with the four dihedrals.

7. PHASE II BEAM COMBINER

‘OHANA Phase II is designed to be operated in three near-infrared bands: J, H and K. These bands are a compromise between the availability of high-transmission single-mode fibers and the performance of adaptive optics systems. Besides, these bands are of interest for the science targets of ‘OHANA.

‘OHANA making use of single-mode fibers is a monomode interferometer. Its instantaneous field is limited to the Airy pattern and beams are perfectly spatially filtered. Spatial phase errors induced by either atmospheric turbulence or by static aberrations are traded against intensity fluctuations. These need to be monitored to calibrate the interferograms and stabilize fringe contrasts.

FLUOR is the classical set-up to achieve this single-mode calibration (see e.g. Coudé du Foresto et al. 1998¹⁰ and Perrin et al. 1998¹¹). The triple coupler provides the two complementary interferometric outputs of a classical Michelson interferometer (beam splitter set-up) and the two photometric outputs proportional to the input filtered intensities. A FLUOR triple coupler is needed for each band of the interferometer. For both technical (longer coherence length) and obvious astrophysical reasons, spectral dispersion is also a requirement. At the time the project got decided, 3 triple couplers could not be afforded. The advantage of the triple coupler was however needed: the simultaneous measurement of the interferometric and photometric signals for accurate calibration of visibilities. This can be achieved with a single coupler if inputs are chopped at different frequencies, the photometric signals and interference fringes being multiplexed at 3 different frequencies and easily retrievable in Fourier space. This however proves to be complex and inefficient in

transmission. The idea of frequency coding has been kept in the ‘OHANA beam combiner but realized differently as illustrated by Figure 7.

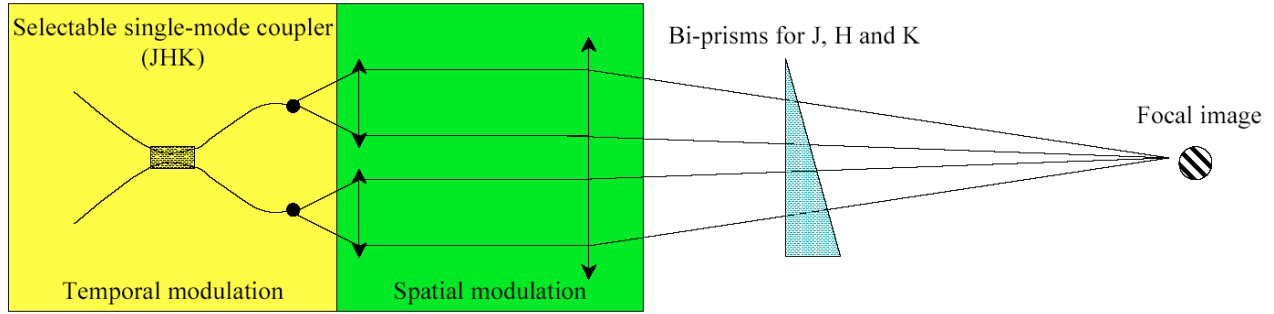


Figure 7: Principle of the ‘OHANA Phase II beam combiner. The beam combiner uses both temporal and spatial modulations. Temporal fringes contain the spatial information on the source. Spatial fringes code the input intensities useful to calibrate the interferogram against turbulence. Fringes in J, H and K’ bands are dispersed.

The beam combiner figures two types of modulations. A temporal modulation which performs the interferometric mixing of the input beams and produces the temporal fringe pattern whose contrast is the spatial information on the source. This part of the beam combiner, a co-axial combiner, is a single-mode coupler, one for each band. Coupler ends are mounted on motorized fiber selectors. The two outputs of the coupler, the two complementary interferograms with respective phase shifts of $-\pi/2$ and $+\pi/2$, feed a multi-axial combiner which performs the mixing in the focal plane at infinity with spatially coded fringes across the diffraction pattern. Each recorded frame is therefore a spatial interferogram. When varying the opd linearly with time, multiple frame scans are recorded and contain both the temporal and the spatial modulation.

For the sake of clarity and simplicity the equation of the recorded signal is presented in the simplified case in which the transmission and reflexion ratios of the coupler are equal to 50%. It also works with real-life unmatched and chromatic ratios. It is also assumed that the beams of the multi-axial beam combiner have equal lengths. Fiber outputs are mounted on translation stages to set the opd of the multi-axial beam combiner to zero. In this case, the expression of the cut of the diffraction pattern in a the direction perpendicular to the spatial fringes is:

$$I(x, \delta, t) = I_0(x) \cdot \left\{ [P_A(t) + P_B(t)] + 2|V|\sqrt{P_A(t)P_B(t)} \cos(2\pi\sigma\delta - \varphi + \varepsilon) \cos(2\pi\sigma dx / f) + [P_A(t) - P_B(t)] \sin(2\pi\sigma dx / f) \right\}$$

where x is the focal plane spatial coordinate, δ is the optical path difference of the co-axial beam combiner, t is time, σ is the wavenumber, ε is the differential piston error, $Ve^{i\varphi}$ the visibility and f the focal length of the camera. P_A and P_B are the filtered intensities at the input of the coupler coming from telescopes A and B. $I_0(x)$ is the cut of the diffraction pattern in the direction perpendicular to the spatial fringe modulation. In practice it is the image collapsed in this direction by an anamorphosis optical system as this direction does not contain any interferometric information. The remarkable property of this multi-co-axial beam combiner is that the sum of the photometric beams, the high resolution spatial information and the difference of the interferometric beams can be separately decoded. In focal space, the sum of the photometries are not modulated whereas the difference of photometries and the visibility are the two quadratures of a spatial carrier wave. Demodulation therefore provides the three following quantities:

- $P_A(t) + P_B(t)$
- $2|V|\sqrt{P_A(t)P_B(t)} \cos(2\pi\sigma\delta - \varphi + \varepsilon)$
- $P_A(t) - P_B(t)$

and eventually the normalized interferogram $|V|\cos(2\pi\sigma\delta - \varphi + \varepsilon)$ free of coherent energy fluctuations.

The beam combiner has been set-up at the IOTA interferometer at the Smithsonian Institution Fred L. Whipple Observatory (Traub et al. 2004¹²). The FLUOR tables and the FLUOR front end optics have been re-used for this purpose. First tests were performed in June 2003 in the K band. A second run took place in October 2003 in both K and H bands. First fringes in K are displayed in Figure 8. The classical fringes (fringes with intensity fluctuations) are displayed along the classical fringes. It is remarkable that the processed fringes are not band-pass filtered and that the intensity low frequency fluctuations have been removed without requiring any filtering.

The ‘OHANA beam combiner also features dispersion with moderate spectral resolution ($R = 300$). The camera of the multi-axial beam combiner is an anamorphic set-up (a Chretien’s hypergonar) which compresses the fringes in the direction orthogonal to the modulation. Bi-prisms for each band are inserted in the beam and disperse the two-fringed beam in this same direction. Tests at IOTA have been carried out to track fringes with the group delay technique, an efficient technique to search fringes in wide band with a long coherence length.

The beam combiner will be used for the Gemini-CFHT baseline. Combination of Keck I and Keck II will be performed with the Keck interferometer K band beam combiner.

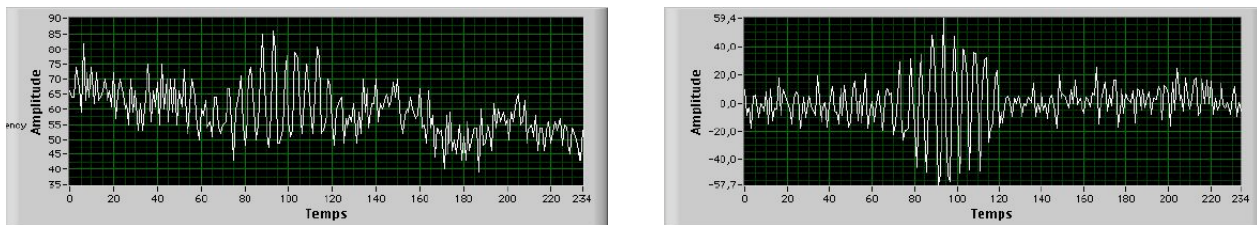


Figure 8: first fringes detected with the ‘OHANA beam combiner at IOTA on ϵ Peg. Left: classical fringes with photometric fluctuations due to filtered turbulent phase. Right: instantaneously normalized interferogram (see text for equations). This is the same signal but processed in two different manners

8. FIRST ‘OHANA BASELINES

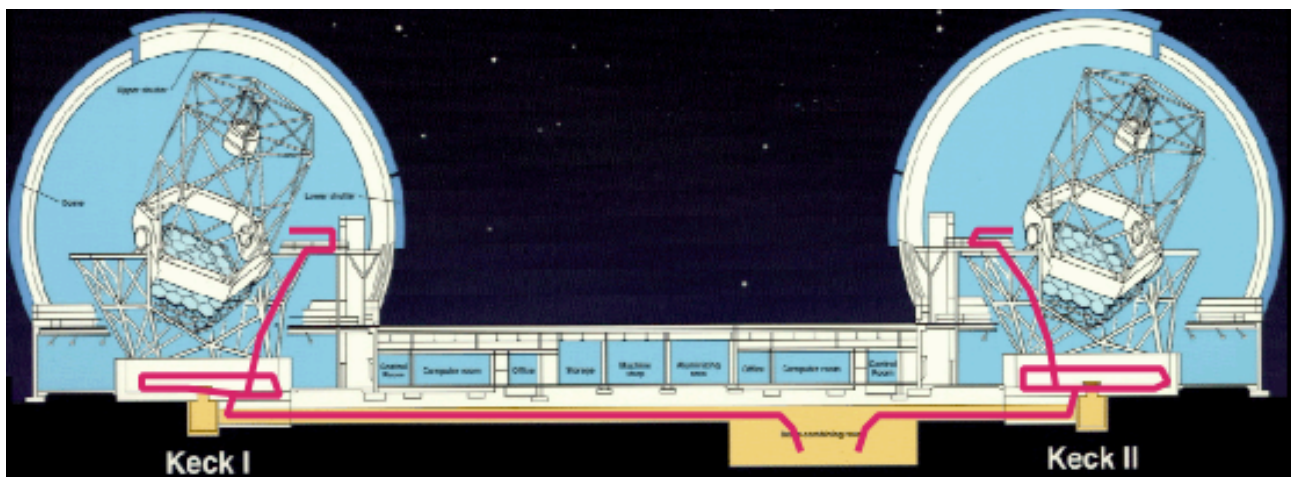


Figure 9: routing of the fibers (in red) for the Keck I – Keck II combination. Light is injected in the fibers at the Nasmyth platforms where adaptative optics systems are located. Fibers reach the entrance of the delay line tunnel through the cable wrap of each telescope so that their integrity is preserved during telescope azimuth rotation. They follow on their route to the beam combining lab where the beams are extracted and launched into the delay lines and beam combiner.

Pairs of three hundred meters of fibers have been balanced in dispersion for the J, H and K bands. This will allow to link baselines up to 450 m in Phase II. Baselines among the “easiest” must be tested first in order to build credit for ‘OHANA. The first baseline will be Keck I – Keck II. The test will occur on the night of December 1st, 2005. Although this one belongs to an existing interferometer¹³, the ‘OHANA fibers will by-pass the interferometer optical train down to the delay lines (see Figure 9). Only the K band fibers will be used for this first baseline as the K band Keck beam combiner will be used to detect fringes. It is to be noticed however that the whole length of fibers is 300 m in each arm that is to say enough to link two telescopes 400 to 500 m apart and this first experiment is therefore indicative of the performance of future long baseline links with large telescopes equipped with adaptive optics systems.

The second baseline will be the Gemini-CFHT baseline in 2005, a typical baseline linking two totally different telescopes not meant for interferometry (see Figure 10). All three bands will be used with the whole ‘OHANA system: injection modules, fiber links, delay line and beam combiner. It is not sure yet how fibers will be routed, either underground or on the ground. The difficulty will be increased compared to the Keck I – Keck II baseline as the baseline vector will have to be measured and put on firm ground after first fringes will have been detected. Also, beam properties will not be symmetric in telescopes possibly causing polarization problems which will have to be solved.

Next baselines are still under discussion as we all expect first results. A tentative schedule for a next combination is 2006 as a new or new injection module(s) will first have to be tested.

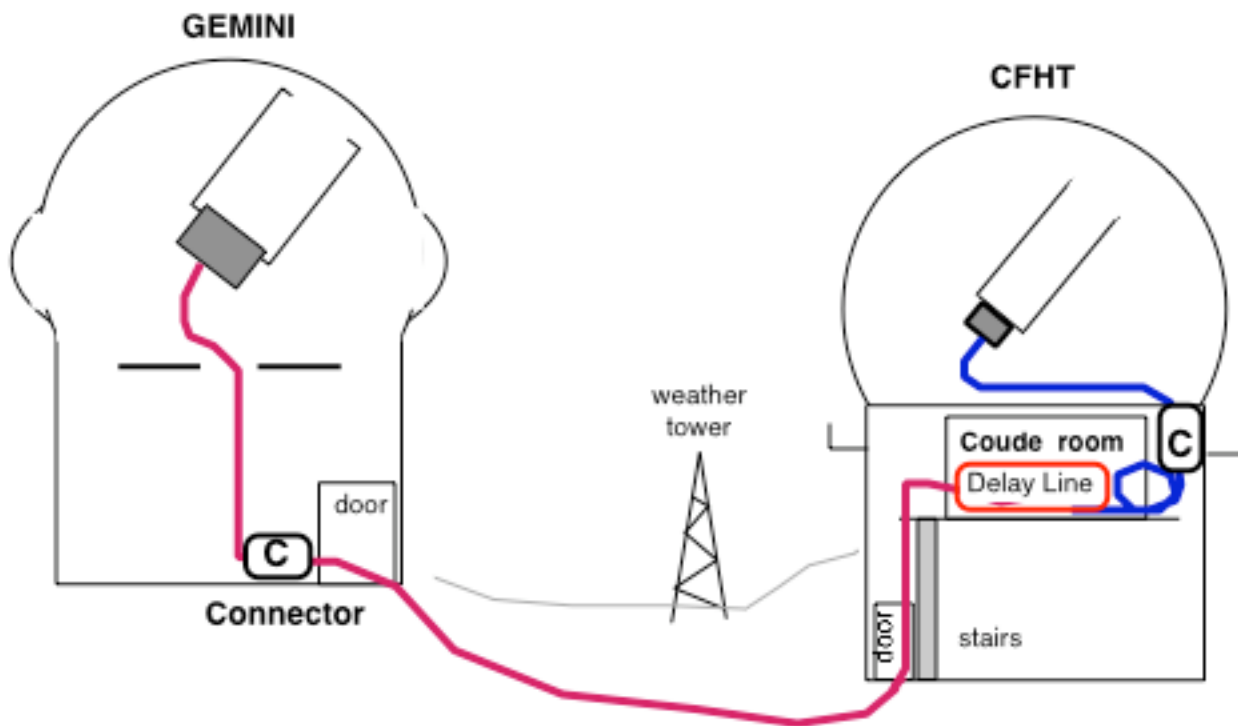


Figure 10: layout of the fibers between CFHT and Gemini. The 300 m fiber cables on the CFHT will hang from the telescope Cassegrain focus and will directly be routed to the Coude room below the telescope where the delay line and beam combiner are located. The fibers from Gemini are in two parts. 100 m going from the Cassegrain focus of the telescope to its enclosure and 200 m linking Gemini to CFHT. The two sections can be disconnected at C in case of necessity.

9. SENSITIVITY AND ASTRONOMICAL PROGRAM

The sensitivity estimate depends on the transmission of the whole system and on the stability of the injection in the fibers. Allowing these two parameters to vary within realistic ranges and assuming $1e^-$ read out noise for the detector (optimistic as of today but 'OHANA is a long term project and the multiple-read technique helps reducing detector read-out noise) a limiting magnitude of $K = 13 \pm 1$ can be derived with the 8 meter telescopes². This estimate is consistent with the results of Phase I as long as injection efficiency is concerned. Other parameters will be refined in Phase II (transmission, sampling frequency). If fringe tracking on an off-axis source is possible in Phase II (not anticipated in the current state of the project) then this limiting magnitude can be extended by 5 magnitudes.

This sensitivity will allow to address programs very similar to that of Keck and VLTI: YSOs, AGNs, brown dwarves, supernovae... and will provide both very complementary and unique data^{14,15,16}. For example, the study of YSOs will benefit a lot from baselines reaching 400 m as they are dramatically needed to disentangle between disk models in the near infrared. More generally, merging these data with the Keck-VLTI data will create continuous data sets which will prove very useful to analyze the complex geometry of these objects.

This still may have read very prospective just a year ago, but VLTI and Keck have now shown the way for this type of science. First results on AGNs clearly demonstrate the potential of near-infrared interferometry and its ability to provide results otherwise unaccessible^{17,18,19}. NGC 4151 was the first AGN observed with an interferometer by Keck. This Seyfert 1 galaxy could not be resolved in the K band with the 85 m long baseline showing that the central object is very compact with a characteristic diameter smaller than 5 mas. NGC 1068 has been observed with MIDI at VLTI in the mid-infrared. The source is clearly resolved. It is a Seyfert 2 with a quasi edge-on dust torus partly or totally masking the central engine. Although the torus is resolved the central source remains pointlike or undetected. Measurements in the K' band with VINCI show that the central part is unresolved and less than 5 mas large. These two cases are interesting as the resolution of 'OHANA will allow to resolve central emitter in the near-infrared and make a new step in the understanding of these objects. 'OHANA-type projects have the potential to open breaches in still mysterious science topics.

ACKNOWLEDGEMENTS

This research is supported by the French Ministry of Research, CNRS, Observatoire de Paris and by the Mauna Kea observatories. GP is grateful to Wes Traub for the 'OHANA beam combiner tests and operations at IOTA.

REFERENCES

1. J.-M. Mariotti et al., "Interferometric connection of large ground-based telescopes", *A&AS* 116, 381, 1996
2. G. Perrin et al., "A fibered large interferometer on top of Mauna Kea: 'OHANA, the Optical Hawaiian Array for Nano-radian Astronomy", *SPIE* 4006, 708, 2000
3. J. Woillez et al., "'OHANA Phase I: adaptive optics and single-mode fiber coupling", these proceedings
4. O. Lai et al., "'OHANA Phase III: scientific operation of an 800-meter Mauna Kea interferometer", *SPIE* 4838, 1296, 2003
5. L.M. Simohamed, F. Reynaud, "A 2 m stroke optical fibre delay line", *Pure Appl. Opt.* 6 No 4, L37, 1997
6. S. Vergnole et al., "Using Photonic Crystal Fibre in the frame of stellar interferometer", these proceedings
7. T. Kotani et al., "K band fibers for the 'OHANA project", these proceedings
8. S. Vergnole et al. "Accurate measurements of differential chromatic dispersion and contrasts in an hectometric silica fibre interferometer in the frame of OHANA project", *Optics Communications* 232, 21, 2004
9. S.T. Ridgway, "Optical delay for OHANA", *SPIE* 4838, 1310, 2003
10. V. Coudé du Foresto et al., "FLUOR fibered instrument at the IOTA interferometer", *SPIE* 3350, 856, 1998
11. G. Perrin et al., "Extension of the effective temperature scale of giants to types later than M6", *A&A* 331, 619, 1998
12. W.A. Traub, et al, "IOTA: recent technology and science", these proceedings
13. M.M. Colavita, P.L. Wizinowich & R.L. Akeson, "Keck Interferometer status and plans" these proceedings

14. O. Lai et al., "OHANA: representative science objectives", SPIE 4838, 1410, 2003
15. J. Woillez et al., "Extragalactic astronomy with the OHANA array", these proceedings
16. F. Ménard et al., "OHANA and star formation: probing deep into the accretion/ejection mechanism", SPIE 4838, 1403, 2003
17. M. Swain et al., "Interferometer Observations of Subparsec-Scale Infrared Emission in the Nucleus of NGC 4151", ApJ 596, L163, 2003
18. W. Jaffe et al., "The central dusty torus in the active nucleus of NGC 1068", Nature 429, L47, 2004
19. M. Wittkowski et al., "VLT/VINCI observations of the nucleus of NGC 1068 using the adaptive optics system MACAO", A&A 418, L39, 2004